

Mechanical characterization of lime-stabilized rammed earth: lime content and strength development

Fernando Ávila^{a,*}, Esther Puertas^a, Rafael Gallego^a

^a*Dept. of Structural Mechanics and Hydraulic Engineering, University of Granada, Av. Fuentenueva, 18001 Granada, Spain*

Abstract

Earth construction techniques, such as rammed earth, are present worldwide due to the availability of the material and its mechanical performance. Today they are also attracting attention as an environmentally friendly way of building, although additivition is usually needed. Lime stabilization is an interesting option with long tradition, well-known capacity to improve soil properties and limited environmental impact. This study evaluates the effect of increasing lime contents in the compressive strength and stiffness of rammed earth, and analyses the strength development process of the material. Carbonation depth and ultrasonic pulse velocity are also evaluated due to their relationship with the mechanical behavior. The results show that 12% lime maximized the compressive strength and stiffness of the rammed earth material; the strength was mostly developed during the first month but needs over a hundred days to be fully developed. A good linear correlation between the ultrasonic pulse velocity and the compressive strength is observed.

Keywords: rammed earth, lime stabilization, strength development, mechanical characterization, carbonation, ultrasonic pulse velocity

1. Introduction

The construction sector, nowadays, is well aware of the severe environmental impact caused by its activities, including resource consumption, waste generation and pollution. This situation, which is getting worse over the years due to the increasing demand for housing as the global population grows, has drawn the attention of builders and researchers to non-conventional construction techniques and materials with lower environmental impacts. One such technique, with very long tradition and a promising future, is rammed earth (RE) [1–4].

*Corresponding author

Email addresses: favila@ugr.es (Fernando Ávila), epuertas@ugr.es (Esther Puertas), gallego@ugr.es (Rafael Gallego)

9 RE building technique consist of compacting, between formwork, 7 to 15 cm-
10 thick layers of sandy soil mixed with a certain amount of water in order to create
11 walls with a thickness of 30–60 cm [5–8]. Natural soil can be directly used to
12 build RE structures, leading to the so-called unstabilized rammed earth (URE),
13 with clay acting as the only binder; but when higher strength or durability are
14 required it is common to add different kinds of additives to the mixture. This
15 technique is called stabilized rammed earth (SRE).

16 One of the additives with longest tradition for rammed earth stabilization is
17 lime, existing several examples of historic constructions made of lime-stabilized
18 rammed earth (LSRE) [6, 9–13]. The RE used in these heritage buildings usually
19 contained very significant percentages of lime, e.g., between 10 % and 15 % in the
20 medieval walls of Seville (Spain) [14] and in traditional RE houses in Southern
21 Portugal [15], 20 % in the Alcazaba Qadima and the Alhambra of Granada
22 (Spain) [10, 16], also 20 % in the Saadian sugar refinery of Chichaoua (Morocco)
23 [9], and ca. 25 % in the Fujian Tulou (China) [17] or in the Cáceres city walls
24 (Spain) [14].

25 There is also a broad consensus that lime stabilization improves the me-
26 chanical and hydraulic behavior of soils [18–22]. When lime is added to a soil,
27 the concentration of Ca^{2+} and OH^- increases due to the hydration reaction of
28 lime. This generates the flocculation of particles (affecting soil plasticity) and
29 increases the pH, causing the dissolution of silica and alumina from soil minerals,
30 which react with calcium forming calcium silicate (or aluminate) hydrates that
31 cement soil particles and increase the mechanical performance of the material
32 [19, 23, 24].

33 However, and despite its historical use, today lime has been superseded
34 by cement as the most common stabilizer for rammed earth [25], and as a
35 consequence there is a lack of scientific research specifically analyzing the effects
36 of lime stabilization in the mechanical properties of RE. Ciancio et al. [7] carried
37 out a study evaluating the optimum lime content for LSRE, obtaining a value
38 equal to 4 % by weight, but lime contents greater than 6 % were not considered.
39 Da Rocha et al. [26] also analyzed LSRE materials, from 3 %wt to 9 %wt,
40 concluding that the uniaxial compressive strength increased with increasing lime
41 contents and indicating the need of long curing times. Also Canivell et al.
42 [27] and Arto et al. [28] have recently evaluated the compressive strength and
43 fracture energy, respectively, of RE materials stabilized with high percentages
44 of lime.

45 Understanding the mechanical behavior of LSRE is essential in order to prop-
46 erly preserve the large number of heritage buildings made with this technique,
47 but also because of its potential benefits in the development of an environmentally-
48 friendly way of constructing. Lime is considered to be a much less energy-
49 intensive binder compared to the frequently used Portland cement [7], as its
50 manufacturing temperature is significantly lower (ca. 900 °C as opposed to
51 1500 °C) [29], which reduces the CO_2 emissions during production. It is es-
52 timated that ca. 0.9 t of CO_2 are produced per tonne of cement, while the
53 manufacturing process of lime produces less than 0.7 t of CO_2 per tonne of lime
54 [30–33]. In addition, the carbonation reaction (through which lime uptakes

55 atmospheric CO₂) during the lifetime of the building can counterbalance the
56 carbon emissions generated in the manufacturing and transportation process,
57 leading to a reduction of the net carbon footprint of lime-stabilized materials
58 [29, 34, 35].

59 Against this background, this study presents an analysis of the effect of
60 lime stabilization in the mechanical behavior of rammed earth, evaluating the
61 compressive strength and stiffness of the material with diverse lime contents
62 and analyzing its strength development process.

63 2. Materials

64 2.1. Soil

65 The main source material used for the RE in this study was a natural soil
66 from a quarry in Padul (Granada, Spain), classified according to the European
67 Soil Classification System (ESCS, ISO 14688-2:2018) as clayey well-graded sand,
68 after been passed through a 10 mm sieve in order to remove the coarser parti-
69 cles. The particle size distribution of the resulting earthen material is shown in
70 Figure 1, been in agreement with recent studies regarding rammed earth stabi-
71 lization [36–38] and fitting withing the envelope recommended by Houben et al.
72 [39], widely accepted for URE construction and frequently used also for SRE
73 [25]. The soil had chloride and sulfate contents lower than 0.002 % and was free
74 of organic matter and light contaminants. This soil can be considered to be
75 representative of the material traditionally used in RE construction in Southern
76 Spain [13, 14, 16, 28, 40].

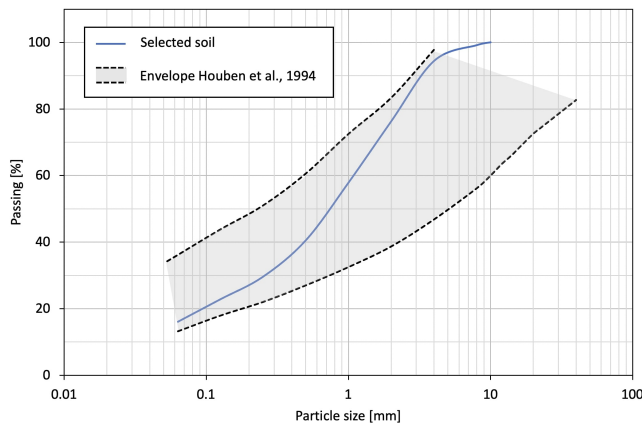


Figure 1: Particle size distribution of the soil.

77 2.2. Lime

78 Natural hydraulic lime with minimum compressive strength of 3.5 MPa at
79 28 days, referred to as NHL 3.5 according to European standard EN 459-1:2015,

80 was used as stabilizer. The main components of NHL are portlandite, reactive
 81 silicates and aluminates formed during calcination from the reaction of crushed
 82 limestone containing clay or other impurities. Table 1 shows the most relevant
 chemical and physical properties of the lime used in the present study.

Parameter	Avg. value
SO ₃ [%]	1.7
Free lime, Ca(OH) ₂ [%]	30
Free H ₂ O [%]	0.7
Residual at 90 μm [%]	5.7
Residual at 200 μm [%]	0.8
Bulk density [kg/dm ³]	0.671
Real density [kg/cm ³]	2.51
Blaine value [cm ² /g]	8500
Setting time [min]	296
End of taking [min]	438
Compressive strength at 28 days [MPa]	4.8

Table 1: Chemical and physical properties of the natural hydraulic lime used in the study, as indicated by the manufacturer.

83

84 3. Experimental procedure

85 3.1. Specimen preparation

86 In order to perform the experimental tests, 10 cm-side cubic LSRE specimens
 87 were manufactured. It is generally assumed that the size and shape of the
 88 samples may affect the mechanical properties obtained [5], although the relation
 89 between these parameters is still unclear and it is out of the scope of this paper.
 90 Similar geometries to the one used for the samples in the present study have
 91 been previously used by several authors [3, 27, 36, 41–44].

92 In order to define the correct amount of water to be added to the mixture,
 93 Modified Proctor tests (UNE 103501 [45]) were performed on specimens with
 94 diverse lime contents. Modified Proctor is a widely established and easily re-
 95 peatable test that provides a compactive effort very close to the one that might
 96 be applied in the construction of a real wall [7, 41]. It was observed that greater
 97 amounts of water were needed in order to obtain the maximum dry density
 98 (MDD) with increasing lime contents, that is to say, the optimum moisture con-
 99 tent (OMC) linearly increased with the lime content. However, this increase in
 100 the OMC with the lime content is quite small (equal to ca. 3%), as it was noted
 101 by Ciancio et al. [7], that reported variations lower than 2% for lime contents
 102 between 0% and 6%. Furthermore, other authors [26, 46, 47] propose using
 103 constant OMC regardless the lime content, as they indicate that the variation
 104 is negligible. The results of the compaction tests also showed that the MDD
 105 of the LSRE decreases with the increase in lime content, in a very pronounced

106 way for small lime contents and then gradually stabilizing. The variation of the
 107 OMC and MDD as a function of the lime content is shown in Figure 2.

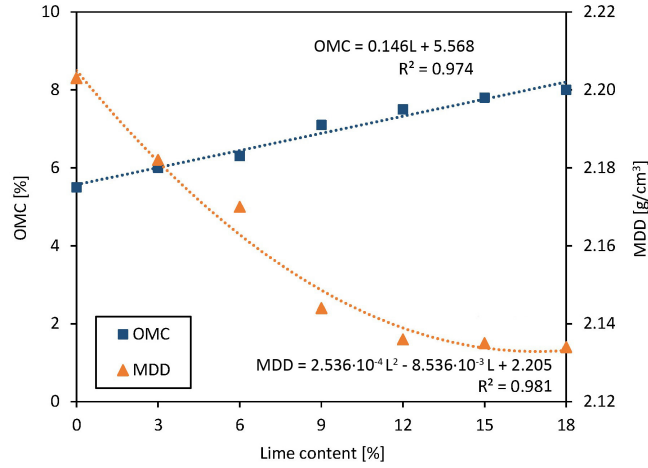


Figure 2: Optimum moisture content and maximum dry density, from Proctor test, as a function of the lime content.

108 The material was prepared by uniformly mixing the natural soil with a certain
 109 amount of lime. Water was added to the mixture until reaching a water
 110 content equal to the OMC+2 %, following the recommendations of Walker et
 111 al. [4] and the New Zealand Standard NZS-4298 [48].

112 The mixture was then poured into cubic molds and compacted by layers of
 113 ca. 2 cm, so each specimen was made up of five earth layers. The small thick-
 114 ness of the layers was chosen in order to provide a more uniform compaction
 115 and to reach a high compaction level by manual means. The material was com-
 116 pacted to 98 % of the MDD, according to NZS.4298 [48]. Once the upper layer
 117 was compacted and its surface smoothed, the samples were carefully removed
 118 from the mold and stored on wire racks, so all the faces could be in contact
 119 with the environment. The specimens were cured under constant conditions of
 120 about 25 °C and 40 % relative humidity, replicating common natural ambient
 121 conditions in Southern Spain.



Figure 3: Some of the LSRE specimens, with different lime contents, stored on wire racks during the curing period.

122 *3.2. Experimental evaluation*

123 The uniaxial compressive strength (UCS) and stiffness of the LSRE spec-
124 imens were determined performing uniaxial compression tests, applying a ho-
125 mogeneously distributed load on the upper face of the sample, perpendicular to
126 the direction of the earth layers. The tests, in the absence of specific standards
127 for RE testing, were performed according to European Standard EN 12390-3
128 “Testing hardened concrete. Part 3: Compressive strength of test specimens”
129 [49]. A linear variable differential transformer (LVDT) was used to measure the
130 longitudinal displacements for the calculation of the stiffness modulus. In the
131 first part of the study, UCS tests were carried out on specimens with increasing
132 lime contents, from 0% to 18% every 3%.

133 Once the results were evaluated, more samples were manufactured with the
134 lime content that led to a better mechanical performance (i.e. 12%). These
135 specimens were subjected to UCS tests at different curing times, from 2 to 100
136 days, with a minimum of three specimens per curing time. The time intervals
137 between the tests were smaller during the first weeks (every 2–5 days), as a
138 greater variation of the mechanical properties was expected –and observed–,
139 and longer for older specimens (every 10 days approx.). After the compression
140 tests, the depth of the carbonation front in the specimens was measured by
141 using phenolphthalein solution 1% in ethanol as indicator, carefully cleaning
142 the surfaces before testing using a compressed air gun. The carbonation depth
143 is measured using a sliding gauge at 3 to 5 equidistant points on each of the
144 four faces on a slice of the specimen, perpendicularly to the exposed surface of
145 the cube, as indicated in standard EN-12390-12 [50]. The carbonation depth
146 considered to be representative of the specimen was obtained as the average of
147 those measurements.

148 During the curing period, the specimens were periodically weighted to control
149 the loss of moisture, and subjected to ultrasonic pulse velocity (UPV) tests.
150 UPV method is one of the non-destructive testing techniques whit a longest
151 tradition for assessing the mechanical properties and inner cracks of building
152 materials. A ultrasonic device, consisting of a transmitting and a receiving
153 transducer, was used to measure the time of pulse of ultrasonic waves over a
154 known path length [51]. Although UPV method has been widely used for con-
155 crete, metal of wooden materials, only a few recent studies have applied it to
156 determine RE mechanical properties [27, 43]. The UPV was measured for the
157 manufactured LSRE specimens in a direction parallel to the earth layers.

158 **4. Results and discussion**

159 *4.1. Stress-strain behavior*

160 The compressive behavior of RE specimens was obtained from the com-
161 pression tests carried out according to standard EN 12390-3 [52], as mentioned
162 above. This standard indicates that the results of the tests can be considered
163 valid if all four exposed faces are cracked approximately equally, generally with
164 little damage to faces in contact with the platens, as shown in Figure 4.



Figure 4: Satisfactory failures of cubic specimens, according to EN 12390-3 [52].

165 Stress-strain curves were obtained from uniaxial compression tests for the
 166 specimens with different lime contents after 28 days of curing. Figure 5 shows
 167 the stress-strain curves of all tested samples. It is possible to observe that, for
 168 almost all the specimens, at the beginning of the test, the material suffers sig-
 169 nificant strains for small load increments, while the earth particles are settling
 170 and so the fine grains fill the empty spaces between the coarser ones. Then,
 171 at ca. 0.01 mm/mm strain, the stiffness significantly increases and the material
 172 shows linear behavior until approximately 75 % of the maximum stress. This
 173 linear phase, however, also comprises plasticity due to the formation of microc-
 174 racks, so it cannot be considered as linear-elastic [47, 53–55]. This is followed by
 175 a plastic phase with a reduction of the stiffness until maximum stress is reached,
 176 then crack propagation occurs rapidly until failure.

177 4.2. Compressive strength and stiffness

According to the evaluation of the stress-strain curves obtained from the
 experimental tests, the material shows a linear behavior approximately between
 35 % and 75 % of the maximum stress, so the stiffness modulus (E) of the
 samples was calculated according to the following equation, which is based on
 the formulation proposed in ASTM C469 [56] for concrete samples, and used
 for rammed earth in previous studies [36, 38]:

$$E = (S_{75} - S_{35}) / (\varepsilon_{75} - \varepsilon_{35}) \quad (1)$$

178 where S_{35} and S_{75} are the stresses corresponding to 35 % and 75 % of the maxi-
 179 mum stress, respectively; and ε_{35} and ε_{75} are the longitudinal strains produced
 180 by stresses S_{35} and S_{75} , respectively.

181 The parameter E defined in Equation 1 is a secant stiffness modulus, fol-
 182 lowing the recommendation of the aforementioned standard and Koutous and
 183 Hilali [47], which indicates that the secant modulus is the best parameter to
 184 describe the elastoplastic mechanical behavior of earthen materials. These au-
 185 thors also noted that the value of the secant modulus is equal to approximately

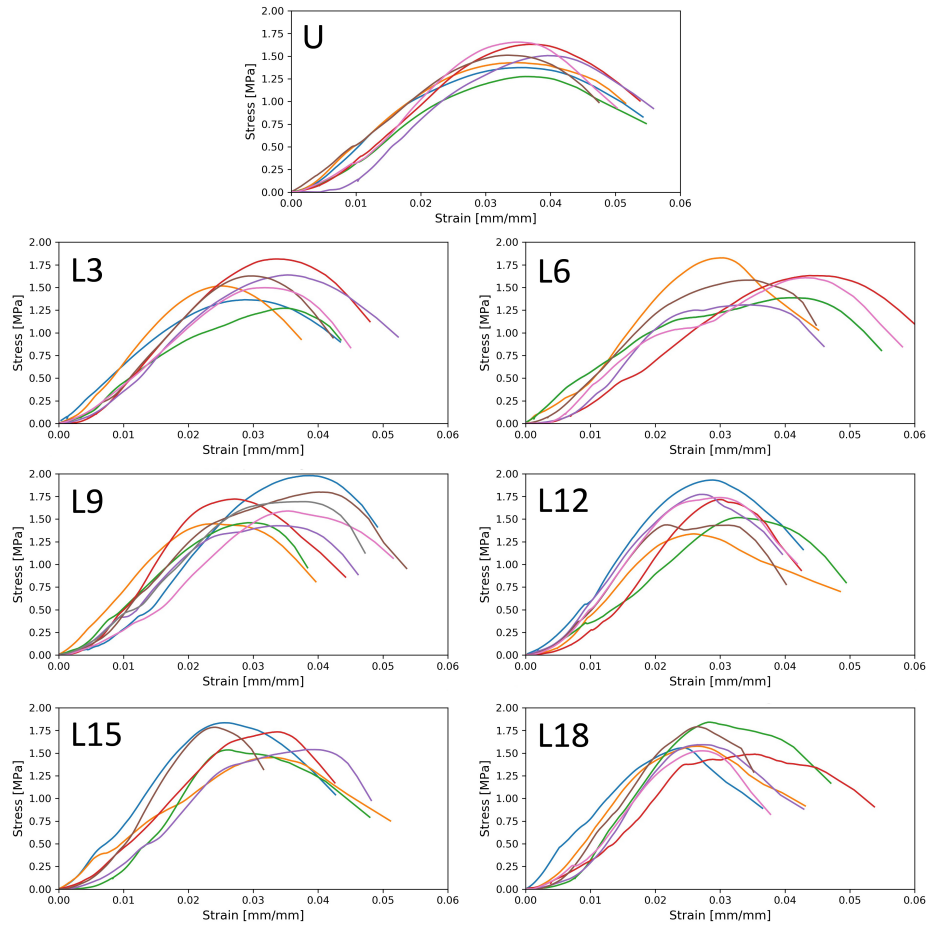


Figure 5: Stress-strain behavior of RE specimens with diverse lime contents at day 28.

186 0.62 times the initial tangent modulus for unstabilized, cement-stabilized and
 187 lime-stabilized rammed earth.

188 Table 2 shows the main results obtained from the uniaxial compressive tests
 189 for each lime content evaluated. The average coefficient of variation (CV) is
 190 equal to 11.0% for the UCS and 17.4% for the stiffness modulus. These values
 191 are reasonable taking into account the intrinsic heterogeneity of the material,
 192 and are comparable (and slightly lower) to the CV presented for SRE in previous
 193 studies [38, 57].

194 It is possible to observe that an increase in the lime content increased the
 195 UCS and E of the RE specimens and decreased the strain reached at maximum
 196 stress. The UCS at 28 days obtained for U specimens is comparable to the
 197 values commonly obtained for URE [5], and was increased by about 11% when
 198 adding 9% of lime, while larger lime contents did not seem to provide greater

Spec.	UCS [MPa]		E [MPa]		ε_c [mm/mm]	
U	1.48	(9.3 %)	64.97	(9.8 %)	0.036	(5.5 %)
L3	1.53	(11.9 %)	73.43	(18.0 %)	0.031	(11.8 %)
L6	1.56	(13.2 %)	72.99	(21.5 %)	0.038	(13.5 %)
L9	1.64	(11.9 %)	81.49	(16.9 %)	0.033	(17.8 %)
L12	1.64	(12.8 %)	91.01	(17.0 %)	0.028	(12.4 %)
L15	1.65	(9.6 %)	92.56	(26.5 %)	0.030	(18.9 %)
L18	1.63	(8.5 %)	93.45	(12.2 %)	0.028	(12.7 %)

Table 2: Uniaxial compressive strength (UCS), stiffness modulus (E) and strain at max. stress (ε_c) obtained for URE and LSRE specimens after 28 days of curing. Coefficient of variation in parenthesis.

199 strength. The reason why increasing lime contents did not improved strength is
200 probably indicating that above that critical lime content there is an insufficient
201 amount of aluminosilicate material in the soil to support additional stabilization
202 reactions with the lime.

203 The UCS results obtained in the present study have been compared with
204 those ones reported in literature, although the latter are very scarce and present
205 a great dispersion. Ciancio et al. [7] obtained higher improvements (ca. 70 %) in
206 the UCS with an optimum lime content of 4 %, but the initial strength for URE
207 was extremely low (0.70 MPa), and so it was the maximum strength reached
208 adding lime. Arto Torres [58] also performed compression tests on 10 cm-side
209 cubic samples, with very high lime contents –20 and 25 %vol–, obtaining UCS
210 equal to 2.64 MPa and 2.38 MPa, respectively. A similar dosage (18 %vol lime)
211 was used by Canivell et al. [27], obtaining an average compressive strength of
212 1.87 MPa. Not very different results were obtained by Koutous and Hilali [47],
213 leading to UCS between 1.58 MPa and 2.55 MPa for 4%-LSRE specimens. Da
214 Rocha et al. [26] also evaluated the UCS of LSRE, obtaining surprisingly low
215 values (under 1.00 MPa for all lime contents from 3 to 9 %). Despite of the
216 differences, two aspects observed in the present study were also noted by [26]:
217 UCS increases as the lime content increases and UCS increases as the curing
218 time increases.

219 The huge differences in the results showed in the diverse studies regarding
220 lime stabilization of RE make it very difficult to draw general conclusions, so it
221 would be necessary to carry out specific tests for particular soils and ambient
222 conditions in order to assess the optimum lime content for the compressive
223 strength and the maximum value of this parameter for each RE construction
224 under consideration. If a range of UCS of LSRE should be established to have
225 an order of magnitude, it would be from 1.00 to 2.50 MPa, a range in which the
226 results of the present study fit.

227 Regarding the elastic (secant) modulus, the values obtained in the present
228 study for the URE specimens are in agreement with those proposed by Mania-
229 tidis and Walker [59] and Bui and Morel [1]. Some other studies propose higher
230 E values [38, 41, 60], but the enormous dispersion in the results presented in

231 literature regarding this parameter does not allow to define a value of consensus
 232 [5, 25]. Considering the studies specifically evaluating LSRE, only Ciancio et al.
 233 [7] indicates the measurement of the stiffness, showing values between 150 MPa
 234 to 200 MPa. Again, the lack of results in literature and their variability make
 235 it very difficult to draw conclusions about this parameter.

236 Analyzing the variation of the stiffness when adding different lime contents,
 237 it can be observed that no relevant increases were obtained with lime contents
 238 lower than 9%, but it significantly improved (about 25%) when reaching that
 239 lime content. The increase in the secant stiffness modulus was even higher
 240 (over 40%) for L12 specimens and then remained approximately constant when
 241 higher percentages of lime were added. The significance of these stiffness im-
 242 provements is assessed through an ANOVA test, obtaining a p-value of 0.003,
 243 much lower than the significance level (0.05), which provides strong evidence to
 244 conclude that the population means —mean stiffness for each lime content—
 245 are significantly different. Figure 6 shows the evolution of the stiffness with the
 246 lime content, together with the variation of the compressive strength.

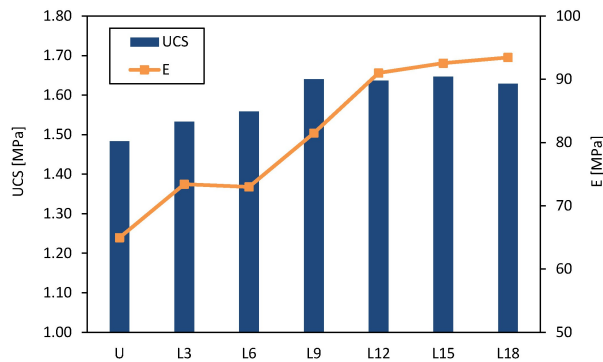


Figure 6: Average uniaxial compressive strength and stiffness for increasing lime contents at day 28 (Table 2).

In the second part of the study, UCS tests were repeated for 12%-LSRE specimens, as it was observed that this lime content was the limit over which the improvements in the mechanical properties was almost negligible. The tests performed for the L12 specimens evaluated the strength development process for this SRE material. The results show an exponential evolution of the UCS of the specimens along time (Figure 7); Equation 2 is proposed as the expression that fits better the evolution of the UCS of the LSRE specimens over time, with a coefficient of determination $R^2 = 0.82$.

$$\text{UCS} = 2.530 (1 - \exp(-0.386 t^{0.277})) \quad (2)$$

247 whic UCS in MPa and the curing time, t , in days.

248 These results and the proposed equation indicates a maximum UCS of
 249 2.53 MPa at infinite time. Sixty five percent of this maximum strength is devel-
 250 oped during the first 28 days of curing, and this percentage increases to 75%

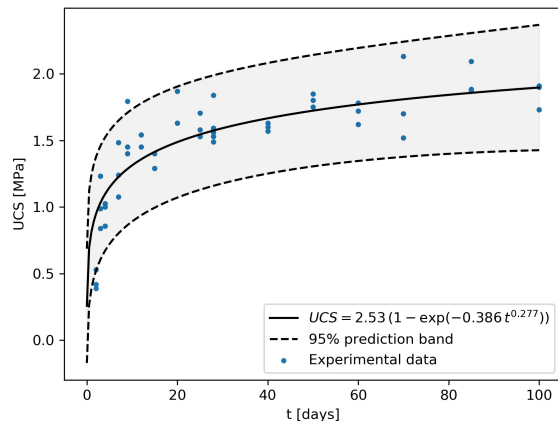


Figure 7: Development of the uniaxial compressive strength over time for L12 specimens.

251 if waiting until day 100. Although the UCS values obtained for 12%-LSRE in
 252 the present study —1.64 MPa at day 28 and 1.89 MPa at day 100— are not
 253 particularly high if compared with some of the most recent results in literature
 254 that stabilize RE with diverse combinations of additives (most of them includ-
 255 ing cement), they are in agreement with most studies considering RE stabilized
 256 only or mainly with lime, as mentioned above.

257 Regarding the strength development process, it is common in literature to
 258 analyze the UCS of RE at relatively short periods of time (usually 28 days
 259 [7, 27, 58]), despite the fact that it is well known that the strength develop-
 260 ment of lime-stabilized earth is a long-term process [20, 22, 24]. In fact, some
 261 studies regarding LSRE [18, 26] indicate that the UCS of the material is still
 262 increasing after 100–360 days of curing. In order to reduce these long curing
 263 periods, Da Rocha et al. [26] proposed limiting the lime content and including
 264 a significant percentage of fly ash (over 25%). There are also some examples
 265 of ancient LSRE structures constructed centuries ago that may help indicating
 266 the potential strength of this material at “infinite” time; this is the case of the
 267 Tower of Comares at the Alhambra (Granada, Spain), where cylindrical samples
 268 were extracted from its walls and tested in laboratory obtaining a compressive
 269 strength of 2.45 MPa [10, 61].

270 It is well known, therefore, that the strength acquisition process is slow and
 271 requires a significant amount of time to be fully developed. However, it is also
 272 possible to observe that a huge percentage of the final strength is developed
 273 during the first weeks of curing, due to the hydration reaction of lime that
 274 starts just after the lime is added to the soil in the presence of water. It was also
 275 observed that, during the first ten days of curing, the weight of the specimens
 276 significantly decreased, mainly due to the evaporation of the water present in the
 277 mixture, and then remained almost completely constant. The weight variation

278 of the samples during their first month of curing is shown in Figure 8. A similar
 279 behavior of the moisture loss process was observed by Arto et al. [28] for LSRE
 280 specimens cured in natural ambient conditions. Curing conditions with higher
 281 relative humidity could reduce evaporation and extend the hydration process of
 282 lime, prolonging the time required for the strength to stabilized and allowing
 283 the material to reach higher strength values.

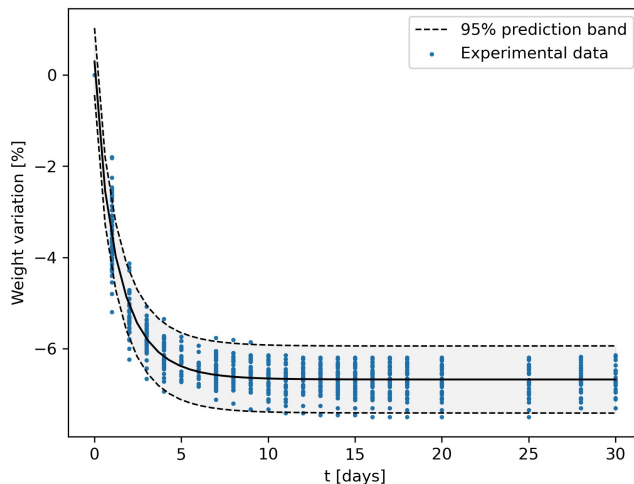


Figure 8: Weight variation of L12 specimens during the first 30 days of curing.

284 Evaluating the stiffness modulus, it is possible to observe the existence of a
 285 linear correlation between this parameter and the UCS of the LSRE specimens,
 286 where E is equal to ca. 57 times the UCS with $R^2 = 0.75$, as shown in Figure 9.
 287 A linear relationship between these two parameters has been noted in several
 288 previous studies regarding RE with diverse stabilizers [36, 38, 59, 62, 63]. Some
 289 relevant earth construction standards, such as NZS 4297 [64], also indicate that
 290 the stiffness can be linearly obtained from the UCS values if there is not more
 291 specific data.

292 4.3. Carbonation

293 It is also useful to evaluate the evolution of the carbonation depth in the
 294 LSRE specimens, as it is closely related to the strength development process
 295 [35]. Carbonation occurs when the lime added to the soil reacts with the CO_2
 296 present in the air. This phenomenon should generally be avoided, as it subtracts
 297 the lime to other lime-soil reactions and hence inhibits or limits the formation
 298 of cementitious products, reducing the maximum potential strength [19, 24].
 299 Although carbonation speed could be slowed down by limiting the CO_2 con-
 300 centrations in the curing environment, this is unlikely to be possible in a real
 301 construction site, so natural ambient conditions were considered in the present
 302 study.

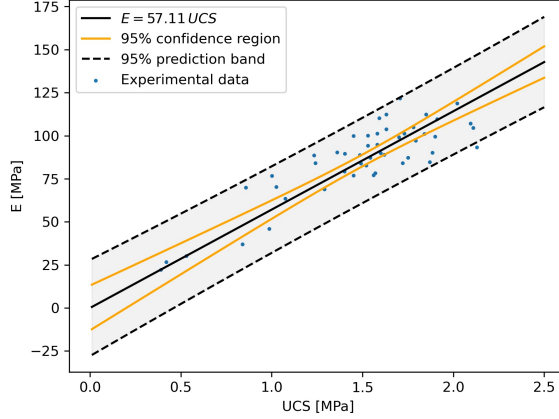


Figure 9: Stiffness modulus as a function of the uniaxial compressive strength.

The carbonation depth in the specimens was measured, after the UCS tests, as the distance between the external faces of the specimen, exposed to carbon dioxide, and the carbonation front. Van Balen and Van Gemert [65] proposed the formula $c = k\sqrt{t}$ to explain the evolution the carbonation depth (c) in lime mortars, where t is the curing time and k is an experimental factor. Basing on this expression and considering the results obtained in the present study, equation 3 is proposed to describe the evolution of the carbonation depth in the 12%-LSRE specimens, with a coefficient of determination equal to 0.93.

$$c = 4.319 t^{0.430} \quad (3)$$

303 where c is the carbonation depth in mm and t is the curing time in days.

304 Although the growth of the carbonate depth is faster during the first days
 305 of curing (Figure 10), as it happens with the strength acquisition or moisture
 306 loss, the carbonation process continues to develop for a much longer time. In
 307 the case of the 100 mm-side cubic specimens used in this study, the samples
 308 would be fully carbonated after ca. 300 days of curing. The carbonation speed
 309 also depends on the lime content, as it can be observed in Table 3, which
 310 includes the carbonation depth of the specimens for diverse lime contents at
 311 day 28, when they were subjected to the UCS tests. The carbonation depth
 312 after 28 days of curing is higher for samples with lower lime contents, probably
 313 because greater lime percentages result in a finer pore structure that impedes
 314 CO₂ permeation [17, 19, 66]. Also, as the amount of carbon dioxide in the
 315 atmosphere is controlled, a greater lime content in the material takes longer
 316 to carbonate and so a reduced carbonation rate occurs with increasing lime
 317 content.

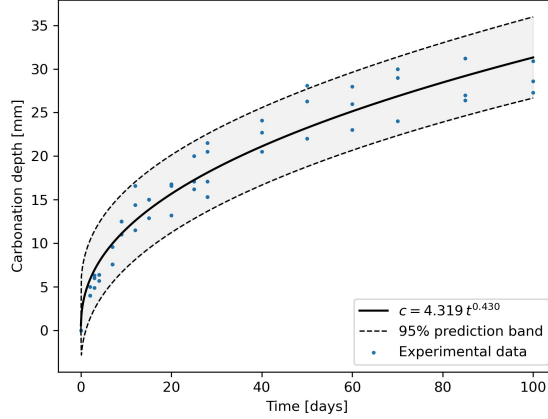


Figure 10: Evolution of the carbonation depth during the curing period.

	L3	L6	L9	L12	L15	L18
c [mm]	32	25	19	18	20	18
C.V. [%]	9.1	7.3	10.7	12.3	9.7	10.7

Table 3: Carbonation depth (c) of LSRE specimens after 28 days of curing. Mean value and coefficient of variation.

318 4.4. Ultrasonic pulse velocity

The UPV through the RE samples was measured before destructive UCS testing in order to assess a potential relationship between this parameter and the mechanical properties of the material. In fact, the analysis of the results shows a linear correlation between the UPV and the UCS of the LSRE specimens, following Equation 4, where UCS is expressed in MPa and UPV in km/s. This relationship and its 95 % prediction band and confidence region are shown in Figure 11.

$$\text{UCS} = -1.416 + 1.897 \text{UPV} \quad (4)$$

319 Although there are very few studies that use the UPV technique for RE ma-
 320 terials, some authors have already indicated the existence of a linear correlation
 321 between compressive strength and ultrasonic pulse velocity [27, 43, 67]. There-
 322 fore, and despite the evident existing dispersion in the values of the mechanical
 323 properties of RE materials, which is partially intrinsic to the heterogeneity of
 324 the material itself [5], the existing relationship between the UCS and the UPV
 325 makes the measurement of the latter a useful method to estimate the mechan-
 326 ical properties without damaging the sample. This can be particularly useful
 327 for existing RE structures, especially in the case of heritage buildings where de-
 328 structive testing techniques cannot be applied. Previous studies have also noted

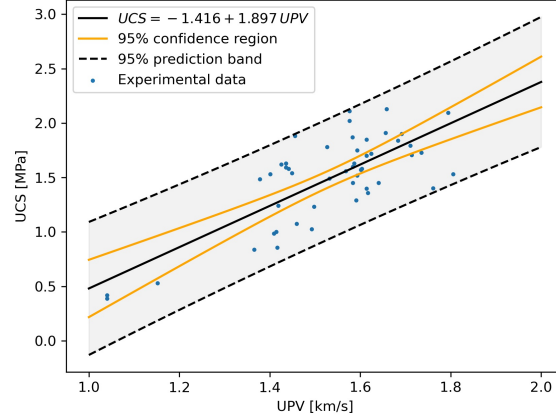


Figure 11: Uniaxial compressive strength as a function of the ultrasonic pulse velocity.

329 the usefulness of the UPV technique to predict the compressive behavior and
 330 to detect damage for other common construction materials, such as concrete
 331 [68, 69] or brick and stone masonry [70, 71].

332 For new constructions, on the other hand, UPV measurements during the
 333 curing period can be used to assess the evolution of the mechanical properties.
 334 A stabilization in the UPV values would indicate the stabilization of the UCT
 335 and stiffness, meaning that the material has already developed the majority of
 336 its strength (initial part of the strength development curve).

337 5. Conclusions

338 Rammed earth is a traditional building technique that is attracting a re-
 339 newed interest due to its low environmental impact and limited construction
 340 costs. Over the last decades, the scientific research regarding RE construction
 341 has been mainly focused on unstabilized or cement-stabilized material, in ad-
 342 dition to some other modern additives. On the other hand, very few studies
 343 have evaluated the mechanical characteristics of RE stabilized with lime, even
 344 though it is a traditional additive widely used in soil stabilization, causing an
 345 environmental impact lower than other common stabilizers such as cement, and
 346 which is present in several historic RE buildings.

347 In the present study, several RE samples with different lime contents and
 348 curing periods have been evaluated in order to analyze the effect of lime sta-
 349 bilization on the mechanical properties of the material. The results show an
 350 increase in the UCS and stiffness when increasing the lime content, in agree-
 351 ment with some other previous studies [7, 26], until a certain percentage of lime from
 352 which no improvement of the mechanical properties was obtained. This strength
 353 standstill is related to the lack of the aluminosilicate material in the soil, so the

354 optimum lime content (minimum lime content for which the maximum strength
355 is reached) may vary depending on the mineralogical characteristics of the soil,
356 so it would be recommended to perform some UCS tests for the specific soil to
357 be used in a construction before choosing the lime content. For the material
358 used in the present study, representative of the soils traditionally used in RE
359 construction in Southern Spain, the optimum lime content for the compressive
360 strength and stiffness was equal to 12%.

361 The mechanical properties of the 12%-LSRE samples were also evaluated
362 during 100 days of curing, observing an exponential evolution of the UCT that
363 shows that a significant percentage of the strength is developed during the first
364 20–30 days, but also indicating that the strength development process could
365 last hundreds of days (about 75% of the predicted strength was reached by day
366 100). Similar behavior was observed for the material stiffness, which showed a
367 linear relationship with the UCS, although the stiffness values showed higher
368 dispersion, also noted in previous studies [25].

369 Also carbonation of the specimens, considered detrimental to strength devel-
370 opment, was evaluated. Carbonation was observed to develop faster in samples
371 with low lime contents, where the coarser pore structure leads to a faster carbon
372 dioxide permeation. This phenomenon, however, occurs in a slower way than
373 other lime-soil reactions, following a potential evolution of the form $c = at^b$.

374 In addition, non-destructive UPV tests were performed. This technique
375 has proved to be a useful method to estimate the mechanical properties of
376 the material without damaging the sample, due to its linear relation with the
377 compressive strength of the material. UPV tests could be easily performed
378 on RE walls in a construction site, where the stabilization in the values obtained
379 could be used as an indicator that the mechanical parameters have also increased
380 and reached a stable value.

381 Declaration of competing interest

382 The authors declare that they have no known competing financial interests or
383 personal relationships that could have appeared to influence the work reported
384 in this paper.

385 Acknowledgments

386 This research was supported by the Spanish Ministry of Universities via a
387 doctoral grant to Fernando Ávila (FPU18/03607).

388 The study is part of the project “*Revalorización Estructural del Patrimonio*
389 *Arquitectónico de Tapial en Andalucía*” (Structural Revaluation of the Rammed
390 Earth Architectural Heritage in Andalusia), ref. A-TEP-182-UGR18, within the
391 framework of the European Regional Development Fund Program of Andalusia
392 2014-2020, and has been carried out by members of the Research Group “Solid
393 Mechanics and Structures” (TEP167) at the Sustainable Engineering Structures
394 Laboratory (SES-Lab) of the University of Granada.

395 **References**

- 396 [1] Q. B. Bui, J. C. Morel, Assessing the anisotropy of rammed earth, *Constr. Build. Mater.*
397 23 (9) (2009) 3005–3011. doi:10.1016/j.conbuildmat.2009.04.011.
- 398 [2] J.-C. Morel, R. Charef, E. Hamard, A. Fabbri, C. Beckett, Q.-B. Bui, Earth as con-
399 struction material in the circular economy context: practitioner perspectives on bar-
400 riers to overcome, *Philos. Trans. R. Soc. B Biol. Sci.* 376 (1834) (2021) 20200182.
401 doi:10.1098/rstb.2020.0182.
- 402 [3] S. S. D. Raavi, D. D. Tripura, Predicting and evaluating the engineering properties of
403 unstabilized and cement stabilized fibre reinforced rammed earth blocks, *Constr. Build.*
404 *Mater.* 262 (2020) 120845. doi:10.1016/j.conbuildmat.2020.120845.
- 405 [4] P. Walker, R. Keable, J. Martin, V. Maniatidis, *Rammed earth : design and construction*
406 *guidelines*, 2005.
- 407 [5] F. Ávila, E. Puertas, R. Gallego, Characterization of the mechanical and physical prop-
408 erties of unstabilized rammed earth: A review, *Constr. Build. Mater.* 270 (2021) 121435.
409 doi:10.1016/j.conbuildmat.2020.121435.
- 410 [6] D. Alex, Recognition of a heritage in danger: Rammed-earth architecture in Lyon city,
411 France, *IOP Conf. Ser. Earth Environ. Sci.* 143 (1) (2018). doi:10.1088/1755-1315/143/
412 1/012054.
- 413 [7] D. Ciancio, C. T. S. Beckett, J. A. H. Carraro, Optimum lime content identification for
414 lime-stabilised rammed earth, *Constr. Build. Mater.* 53 (2014) 59–65. doi:10.1016/j.
415 conbuildmat.2013.11.077.
- 416 [8] R. El Nabouch, Q. B. Bui, O. Plé, P. Perrotin, Assessing the in-plane seismic performance
417 of rammed earth walls by using horizontal loading tests, *Eng. Struct.* 145 (2017) 153–161.
418 doi:10.1016/j.engstruct.2017.05.027.
- 419 [9] N. Gamrani, K. R'kha Chaham, M. Ibnoussina, F. Fratini, L. Rovero, U. Toni-
420 etti, M. Mansori, L. Daoudi, C. Favotto, N. Youbi, The particular "rammed earth"
421 of the Saadian sugar refinery of Chichaoua (XVIth century, Morocco): Mineralogical,
422 chemical and mechanical characteristics, *Environ. Earth Sci.* 66 (2012) 129–140.
423 doi:10.1007/s12665-011-1214-6.
- 424 [10] T. González Limón, M. Álvarez de Buergo, A. de las Casas Gómez, Estudio de los
425 materiales y de las fábricas de la Torre de Comares de la Alhambra, *Cuad. la Alhambra*
426 33-34 (1997) 95–104.
- 427 [11] D. Gandreau, L. Delboy, CRATerre-ENSAG (France), *UNESCO World heritage inven-*
428 *tory of earthen architecture*, 2012.
429 URL <https://unesdoc.unesco.org/ark:/48223/pf0000217020>
- 430 [12] J. Martínez, F. Ávila, E. Puertas, A. Burgos, R. Gallego, Historical and architectural
431 study for the numerical modeling of heritage buildings: the Tower of Comares of the
432 Alhambra (Granada, Spain), *Inf. la Construcción* 74 (565) (2022) e429. doi:10.3989/
433 ic.86683.
- 434 [13] I. Valverde-Espinosa, E. Ontiveros-Ortega, E. Sebastián-Pardo, *El tapial de las murallas*
435 *de Granada*, *Re. Rev. Edif.* 26 (1997) 58–63.
436 URL [https://revistas.unav.edu/index.php/revista-de-edificacion/article/
437 view/34878/30040](https://revistas.unav.edu/index.php/revista-de-edificacion/article/view/34878/30040)
- 438 [14] J. J. Martín-del Río, J. Canivell, M. Torres-González, E. J. Mascort-Albea, R. Romero-
439 Hernández, J. M. Alducin-Ochoa, F. J. Alejandro-Sánchez, Analysis of the materials and
440 state of conservation of the medieval rammed earth walls of Seville (Spain), *J. Build.*
441 *Eng.* 44 (2021) 103381. doi:10.1016/j.job.2021.103381.

- 442 [15] M. I. Gomes, T. D. Gonçalves, P. Faria, Hydric Behavior of Earth Materials and
 443 the Effects of Their Stabilization with Cement or Lime: Study on Repair Mortars
 444 for Historical Rammed Earth Structures, *J. Mater. Civ. Eng.* 28 (7) (2016) 04016041.
 445 [doi:10.1061/\(asce\)mt.1943-5533.0001536](https://doi.org/10.1061/(asce)mt.1943-5533.0001536).
- 446 [16] E. Ontiveros Ortega, E. Sebastián Pardo, I. Valverde Espinosa, F. J. Gallego Roca,
 447 *Estudio de los materiales de construcción de las murallas del Albayzín (Granada)*, PH
 448 Boletín del Inst. Andaluz del Patrim. Histórico 66 (2008) 32–47.
 449 URL <http://hdl.handle.net/11532/245294>
- 450 [17] Y. Luo, H. Zhong, F. Bao, Z. Guo, P. Ni, Insights into natural and carbonation curing
 451 of ancient Chinese rammed earth mixed with brown sugar, *Constr. Build. Mater.* 317
 452 (2022) 125969. [doi:10.1016/j.conbuildmat.2021.125969](https://doi.org/10.1016/j.conbuildmat.2021.125969).
- 453 [18] J. d. J. Arrieta Baldovino, R. L. dos Santos Izzo, E. Batista Moreira, J. Lundgren Rose,
 454 Optimizing the evolution of strength for lime-stabilized rammed soil, *J. Rock Mech.*
 455 *Geotech. Eng.* 11 (2019) 882–891. [doi:10.1016/j.jrmge.2018.10.008](https://doi.org/10.1016/j.jrmge.2018.10.008).
- 456 [19] F. G. Bell, Lime stabilization of clay minerals and soils, *Eng. Geol.* 42 (4) (1996) 223–237.
 457 [doi:10.1016/0013-7952\(96\)00028-2](https://doi.org/10.1016/0013-7952(96)00028-2).
- 458 [20] J. B. Croft, The structures of soils stabilized with cementitious agents, *Eng. Geol.* 2 (2)
 459 (1967) 63–80. [doi:10.1016/0013-7952\(67\)90025-7](https://doi.org/10.1016/0013-7952(67)90025-7).
- 460 [21] G. Deep, Influence of lime and chicken mesh on compaction behaviour and strength
 461 properties of soil, *Mater. Today Proc.* (2020). [doi:10.1016/j.matpr.2020.08.663](https://doi.org/10.1016/j.matpr.2020.08.663).
- 462 [22] S. Islam, N. M. Hoque, M. A. Hoque, P. N. Mishra, M. M. Mamun, S. Dey, Strength
 463 development in fine-grained paddy field soil by lime addition, *J. Build. Eng.* 26 (2019)
 464 100857. [doi:10.1016/j.jobe.2019.100857](https://doi.org/10.1016/j.jobe.2019.100857).
- 465 [23] O. Cuisinier, D. Deneele, F. Masrouri, Shear strength behaviour of compacted clayey
 466 soils percolated with an alkaline solution, *Eng. Geol.* 108 (3-4) (2009) 177–188. [doi:](https://doi.org/10.1016/j.enggeo.2009.07.012)
 467 [10.1016/j.enggeo.2009.07.012](https://doi.org/10.1016/j.enggeo.2009.07.012).
- 468 [24] A. K. Jha, P. V. Sivapullaiah, *Lime Stabilization of Soil: A Physico-Chemical and*
 469 *Micro-Mechanistic Perspective*, *Indian Geotech. J.* 50 (3) (2020) 339–347. [doi:10.1007/](https://doi.org/10.1007/s40098-019-00371-9)
 470 [s40098-019-00371-9](https://doi.org/10.1007/s40098-019-00371-9).
 471 URL <https://doi.org/10.1007/s40098-019-00371-9>
- 472 [25] F. Ávila, E. Puertas, R. Gallego, Characterization of the mechanical and physical prop-
 473 erties of stabilized rammed earth: A review, *Constr. Build. Mater.* 325 (2022) 126693.
 474 [doi:10.1016/j.conbuildmat.2022.126693](https://doi.org/10.1016/j.conbuildmat.2022.126693).
- 475 [26] C. G. Da Rocha, N. C. Consoli, A. Dalla Rosa Johann, Greening stabilized rammed
 476 earth: Devising more sustainable dosages based on strength controlling equations, *J.*
 477 *Clean. Prod.* 66 (2014) 19–26. [doi:10.1016/j.jclepro.2013.11.041](https://doi.org/10.1016/j.jclepro.2013.11.041).
- 478 [27] J. Canivell, J. J. Martín-del Río, F. J. Alejandro, J. García-Heras, A. Jimenez-Aguilar,
 479 Considerations on the physical and mechanical properties of lime-stabilized rammed earth
 480 walls and their evaluation by ultrasonic pulse velocity testing, *Constr. Build. Mater.* 191
 481 (2018) 826–836. [doi:10.1016/j.conbuildmat.2018.09.207](https://doi.org/10.1016/j.conbuildmat.2018.09.207).
- 482 [28] I. Arto, R. Gallego, H. Cifuentes, E. Puertas, M. L. Gutiérrez-Carrillo, Fracture behavior
 483 of rammed earth in historic buildings, *Constr. Build. Mater.* 289 (2021) 123167. [doi:](https://doi.org/10.1016/j.conbuildmat.2021.123167)
 484 [10.1016/j.conbuildmat.2021.123167](https://doi.org/10.1016/j.conbuildmat.2021.123167).
- 485 [29] S.-H. Kang, Y.-H. Kwon, J. Moon, Quantitative analysis of CO₂ uptake and mechanical
 486 properties of air lime-based materials, *Energies* 12 (2019) 2093. [doi:10.3390/en12152903](https://doi.org/10.3390/en12152903).

- 487 [30] CEMBUREAU, *The role of cement in the 2050 low carbon economy*, Tech. rep. (2013).
 488 URL [https://cembureau.eu/media/cpvoin5t/cembureau_2050roadmap_](https://cembureau.eu/media/cpvoin5t/cembureau_2050roadmap_lowcarboneyconomy_2013-09-01.pdf)
 489 [lowcarboneyconomy_2013-09-01.pdf](https://cembureau.eu/media/cpvoin5t/cembureau_2050roadmap_lowcarboneyconomy_2013-09-01.pdf)
- 490 [31] Portland Cement Association, *Carbon footprint*, Think harder. Concr.
 491 URL [https://www.cement.org/docs/default-source/th-paving-pdfs/](https://www.cement.org/docs/default-source/th-paving-pdfs/sustainability/carbon-foot-print.pdf)
 492 [sustainability/carbon-foot-print.pdf](https://www.cement.org/docs/default-source/th-paving-pdfs/sustainability/carbon-foot-print.pdf)
- 493 [32] V. Toufigh, P. Ghassemi, M. Azizmohammadi, M. Ghaemian, H. Rajabi, P. Ghassemi,
 494 Mechanical properties and environmental impact of rubberized fly ash- and red mud-
 495 based geopolymer concrete, *Eur. J. Environ. Civ. Eng.* (2022). doi:10.1080/19648189.
 496 2021.2018358.
- 497 [33] Y. Shan, Z. Liu, D. Guan, CO2 emissions from China’s lime industry, *Appl. Energy* 166
 498 (2016) 245–252. doi:10.1016/j.apenergy.2015.04.091.
- 499 [34] A. J. Edwards, *Properties of Hydraulic and Non-Hydraulic Limes for Use in Construc-*
 500 *tion*, Ph.d. thesis, Napier University (2005).
 501 URL [https://www.napier.ac.uk/\\$\sim\\$/media/worktribe/output-252838/](https://www.napier.ac.uk/\sim/media/worktribe/output-252838/edwardspdf.pdf)
 502 [edwardspdf.pdf](https://www.napier.ac.uk/\sim/media/worktribe/output-252838/edwardspdf.pdf)
- 503 [35] A. El-Turki, R. J. Ball, G. C. Allen, Carbonation of natural hydraulic lime (NHL) 3.5,
 504 in: R. K. Dhir, T. A. Harrison, M. D. Newlands (Eds.), *Cem. Comb. Durable Concr.*,
 505 Thomas Telford Ltd., Dundee, UK, 2005, pp. 300–308.
- 506 [36] M. Kosarimovahhed, V. Toufigh, Sustainable usage of waste materials as stabilizer in
 507 rammed earth structures, *J. Clean. Prod.* 277 (2020) 123279. doi:10.1016/j.jclepro.
 508 2020.123279.
- 509 [37] S. Raj, A. K. Sharma, K. B. Anand, Performance appraisal of coal ash stabilized rammed
 510 earth, *J. Build. Eng.* 18 (2018) 51–57. doi:10.1016/j.jobbe.2018.03.001.
- 511 [38] V. Toufigh, E. Kianfar, The effects of stabilizers on the thermal and the mechanical prop-
 512 erties of rammed earth at various humidities and their environmental impacts, *Constr.*
 513 *Build. Mater.* 200 (2019) 616–629. doi:10.1016/j.conbuildmat.2018.12.050.
- 514 [39] H. Houben, H. Guillaud, *CRAterre*, Intermediate Technology Publications, Earth con-
 515 struction: a comprehensive guide, Intermediate Technology Publications, London, UK,
 516 1994.
- 517 [40] F. J. Alejandro, J. J. Martín del Río, *Caracterización analítica de la muralla tapial*
 518 *almohade de San Juan de Aznalfarache*, in: AHTER-CRIATiC (Ed.), *Construir con*
 519 *tierra ayer y hoy*, V Semin. Iberoam. Construcción con tierra, Mendoza, Argentina, 2006,
 520 p. 119.
 521 URL <https://www.researchgate.net/publication/266014199>
- 522 [41] R. El Nabouch, *Mechanical behavior of rammed earth walls under Pushover tests*, Ph.d.
 523 thesis, Université Grenoble Alpes (2017).
 524 URL <https://tel.archives-ouvertes.fr/tel-01707009/document>
- 525 [42] M. Hall, Y. Djerbib, Rammed earth sample production: Context, recommendations and
 526 consistency, *Constr. Build. Mater.* 18 (4) (2004) 281–286. doi:10.1016/j.conbuildmat.
 527 2003.11.001.
- 528 [43] J. J. Martín-del Río, J. Canivell, R. M. Falcón, The use of non-destructive testing to
 529 evaluate the compressive strength of a lime-stabilised rammed-earth wall: Rebound index
 530 and ultrasonic pulse velocity, *Constr. Build. Mater.* 242 (2020) 118060 Contents. doi:
 531 10.1016/j.conbuildmat.2020.118060.

- 532 [44] D. D. Tripura, K. D. Singh, Characteristic properties of cement-stabilized rammed earth
533 blocks, *J. Mater. Civ. Eng.* 27 (7) (2015) 04014214. doi:10.1061/(ASCE)MT.1943-5533.
534 0001170.
- 535 [45] AENOR, UNE 103501:1994 Geotecnia. Ensayo de compactación. Proctor modificado.
536 (1994).
- 537 [46] M. M. Hallal, S. Sadek, S. S. Najjar, Evaluation of engineering characteristics of stabilized
538 rammed-earth material sourced from natural fines-rich soil, *J. Mater. Civ. Eng.* 30 (11)
539 (2018) 04018273. doi:10.1061/(ASCE)MT.1943-5533.0002481.
- 540 [47] A. Koutous, E. Hilali, Reinforcing rammed earth with plant fibers: A case study, *Case*
541 *Stud. Constr. Mater.* 14 (February) (2021) e00514. doi:10.1016/j.cscm.2021.e00514.
- 542 [48] New Zealand Standard, NZS 4298:1998. *Materials and workmanship for earth buildings*
543 (1998).
544 URL [https://www.standards.govt.nz/sponsored-standards/building-standards/
545 nzs4298/](https://www.standards.govt.nz/sponsored-standards/building-standards/nzs4298/)
- 546 [49] CEN, EN 12390-3. Testing hardening concrete. Part 3: Compressive strength of test
547 specimens (2020).
- 548 [50] CEN, EN 12390-12. Testing hardened concrete. Part 12: Determination of the carbona-
549 tion resistance of concrete. Accelerated carbonation method. (2020).
- 550 [51] S. Kashif Ur Rehman, Z. Ibrahim, S. A. Memon, M. Jameel, Nondestructive test methods
551 for concrete bridges: A review, *Constr. Build. Mater.* 107 (2016) 58–86. doi:10.1016/j.
552 conbuildmat.2015.12.011.
- 553 [52] AENOR. CTN 83 - Hormigón, UNE-EN 12390-3. Ensayos de hormigón endurecido. Parte
554 3: Determinación de la resistencia a compresión de probetas (2020).
- 555 [53] C. T. Beckett, M. R. Hall, C. E. Augarde, Macrostructural changes in compacted earthen
556 construction materials under loading, *Acta Geotech.* 8 (2013) 423–438. doi:10.1007/
557 s11440-012-0203-6.
- 558 [54] H. Fardoun, J. Saliba, N. Saiyouri, Evolution of acoustic emission activity throughout
559 fine recycled aggregate earth concrete under compressive tests, *Theor. Appl. Fract. Mech.*
560 119 (2022) 103365. doi:10.1016/j.tafmec.2022.103365.
- 561 [55] L. Miccoli, D. V. Oliveira, R. A. Silva, U. Müller, L. Schueremans, Static behaviour of
562 rammed earth: experimental testing and finite element modelling, *Mater. Struct. Constr.*
563 48 (10) (2015) 3443–3456. doi:10.1617/s11527-014-0411-7.
- 564 [56] ASTM, C469/C469M Standard Test Method for Static Modulus of Elasticity and Pois-
565 son’s Ratio of Concrete in Compression (2014). doi:10.1520/C0469.
- 566 [57] E. Kianfar, V. Toufigh, Reliability analysis of rammed earth structures, *Constr. Build.*
567 *Mater.* 127 (2016) 884–895. doi:10.1016/j.conbuildmat.2016.10.052.
- 568 [58] I. Arto Torres, *Caracterización mecánica del tapial y su aplicación a estructuras existentes*
569 *mediante el uso de ensayos no destructivos*, Ph.d. thesis, University of Granada (2021).
570 URL <http://hdl.handle.net/10481/69859>
- 571 [59] V. Maniatidis, P. Walker, Structural Capacity of Rammed Earth in Compression, *J.*
572 *Mater. Civ. Eng.* 20 (3) (2008) 230–238. doi:10.1061/(ASCE)0899-1561(2008)20.
- 573 [60] T. T. Bui, Q. B. Bui, A. Limam, S. Maximilien, Failure of rammed earth walls: From
574 observations to quantifications, *Constr. Build. Mater.* 51 (2014) 295–302. doi:10.1016/
575 j.conbuildmat.2013.10.053.

- 576 [61] A. Santos, V. Cuéllar, J. M. Martínez, L. Salinas, [Ground-structure interaction analysis](#)
577 [of the Tower of Comarès, Alhambra of Granada, Spain](#), in: 14th Int. Conf. Soil Mech.
578 Found. Eng., ISSMGE, Hamburg, Germany, 1997, pp. 1025–1028.
579 URL https://www.issmge.org/uploads/publications/1/31/1997_02_0065.pdf
- 580 [62] V. Strazzeri, A. Karrech, M. Elchalakani, [Micromechanics modelling of cement stabilised](#)
581 [rammed earth](#), *Mech. Mater.* 148 (March) (2020) 103540. doi:10.1016/j.mechmat.2020.
582 103540.
583 URL <https://doi.org/10.1016/j.mechmat.2020.103540>
- 584 [63] P. Zare, S. Sheikhi Narani, M. Abbaspour, A. Fahimifar, S. M. Mir Mohammad Hosseini,
585 P. Zare, Experimental investigation of non-stabilized and cement-stabilized rammed earth
586 reinforcement by Waste Tire Textile Fibers (WTFs), *Constr. Build. Mater.* 260 (2020)
587 120432. doi:10.1016/j.conbuildmat.2020.120432.
- 588 [64] New Zealand Standard, [NZS 4297:1998. Engineering design of earth buildings](#) (1998).
589 URL [https://www.standards.govt.nz/sponsored-standards/building-standards/
590 nzs4297/](https://www.standards.govt.nz/sponsored-standards/building-standards/nzs4297/)
- 591 [65] K. Van Balen, D. Van Gemert, Modelling lime mortar carbonation, *Mater. Struct.* 27 (7)
592 (1994) 393–398. doi:10.1007/BF02473442.
- 593 [66] A. Idder, A. Hamouine, B. Labbaci, R. Abdeldjebar, The porosity of stabilized earth
594 blocks with the addition plant fibers of the date palm, *Civ. Eng. J.* 6 (3) (2020) 478–494.
595 doi:10.28991/cej-2020-03091485.
- 596 [67] A. Khan, R. Gupta, M. Garg, Determining material characteristics of “Rammed Earth”
597 using Non-Destructive Test methods for structural design, *Structures* 20 (May) (2019)
598 399–410. doi:10.1016/j.istruc.2019.05.003.
- 599 [68] P. Ghassemi, H. Rajabi, V. Toufigh, Fatigue performance of polymer and ordinary cement
600 concrete under corrosive conditions: A comparative study, *Eng. Fail. Anal.* 111 (2020)
601 104493. doi:10.1016/j.engfailanal.2020.104493.
- 602 [69] P. Ghassemi, V. Toufigh, Durability of epoxy polymer and ordinary cement concrete
603 in aggressive environments, *Constr. Build. Mater.* 234 (2020) 117887. doi:10.1016/j.
604 conbuildmat.2019.117887.
- 605 [70] N. Makoond, L. Pelà, C. Molins, Dynamic elastic properties of brick masonry con-
606 stituents, *Constr. Build. Mater.* 199 (2019) 756–770. doi:10.1016/j.conbuildmat.2018.
607 12.071.
- 608 [71] E. Vasanelli, D. Colangiuli, A. Calia, Z. M. Sbartai, D. Breyse, Combining non-invasive
609 techniques for reliable prediction of soft stone strength in historic masonries, *Constr.*
610 *Build. Mater.* 146 (2017) 744–754. doi:10.1016/j.conbuildmat.2017.04.146.